NPL REPORT ENG **

EMRP SIB-05 DELIVERABLE 1.2.2

HOMOGENEITY AND RESISTANCE OF METAL ON METAL COATINGS

PAUL-ANDRÉ MEURY (LNE), DJILALI BENTOUATI (LNE), JAMES BERRY (NPL), STUART DAVIDSON (NPL), MARK PLIMMER (CNAM) ZACCARIA SILVESTRI (CNAM), MAIJA OJANEN (MIKES), RICHARD HOGSTROM (MIKES), PETER FUCHS (EJPD), KILIAN MARTI (EJPD), JAROSLAV ZUDA (CMI), SEVDA KACMAZ (UME), RICHARD GREEN (NRC)

JUNE 2015

EMRP SIB-05 DELIVERABLE 1.2.2

HOMOGENEITY AND RESISTANCE OF METAL ON METAL COATINGS

STUART DAVIDSON (NPL), JAMES BERRY (NPL),
Engineering Measurement Division

PAUL-ANDRÉ MEURY (LNE), DJILALI BENTOUATI (LNE), JAMES BERRY (NPL), STUART DAVIDSON (NPL), MARK PLIMMER (CNAM) ZACCARIA SILVESTRI (CNAM), MAIJA OJANEN (MIKES), RICHARD HOGSTROM (MIKES), PETER FUCHS (EJPD), KILIAN MARTI (EJPD), JAROSLAV ZUDA (CMI), SEVDA KACMAZ (UME), RICHARD GREEN (NRC)

ISSN XXXX-XXXX

National Physical Laboratory
Hampton Road, Teddington, Middlesex, TW11 0LW

Approved on behalf of NPLML by
Dr Andrew Lewis, Knowledge Leader, Engineering Measurement Division

CONTENTS

1 INTRODUCTION

This document is a report on Deliverable 1.2.2 of EMRP Project SIB05 (NewKILO) The aim of the deliverable was to evaluate the possibility of using composite materials for reference mass standards.

Some composite materials involve surface plating on classical metallic elements or alloys to improve corrosion inhibition, hardness and durability. The aim of coating is to combine the good surface properties of one material with the good bulk properties of another material. In this task, rhodium plating and new methods for applying gold plating on copper (a low permeability material suitable for use with the high magnetic fields involved with watt balance experiments) have been studied. Microscopy has been used to evaluate the efficiency of the method (vapour deposition under vacuum and electroplating) used to deposit the element on surfaces. The porosity of the deposited layer and the interface between the substrate and the coating have been then characterised by microscopy. In addition, the adherence of the coatings was evaluated by indentation.

2 COATING PREPARATION

Gold-electroplated surfaces were produced by both the National Research Council (NRC), Canada and Häfner Gewichte GmbH and rhodium-electroplated surfaces by Häfner alone.

2.1 NRC GOLD PLATED SURFACES

At NRC, copper substrates were electroplated with gold beginning with three different commercial precursor solutions. The three oxygen-free (99.99 %) copper discs used in the study were cut from a rod approximately 10 mm in diameter to a thickness of approximately 0.5 mm. At this point the surface retained a smooth machine finish, but no subsequent polishing was performed. All sample plating was performed in a class 100 clean room within the NRC Institute for Microstructural Sciences.

The precursor solutions tested are not an exhaustive list but were selected to range over different chemistries and pH values. The oxygen free machine finished copper substrates were cleaned to remove oils and thin native oxides but heavier cleaning, polishing or etching to create a more ideal substrate was not performed. Therefore the relative efficacy of the coatings is rated on a local scale and several defects in the coating could be largely influenced by the substrate and could be removed by more extensive substrate preparation. As all substrates were similar, the concentration of defects in the film derived from each precursor indicates the relative sensitivity of the coating to defects in the substrate.

Before plating a 5 step procedure was implemented to clean the substrates, remove machining and hand oils as well as the native oxide layer. In step 1 the sample was placed in an ultrasonic bath of acetone (CMOS grade JT Baker) for 5 minutes, followed by an isopropyl alcohol (Finyte JT Baker) rinse at 80 °C for 5 minutes. In step 3 the sample was rinsed in a two-stage deionized (DI) water cascade in which the resistance of the water in the purest 2nd stage was monitored. The substrate was rinsed for 5 minutes in stage one and about 5 minutes in stage two, until the resistance reached 17 MΩ (i.e. a conductance of 0.06 μS). In step 5 the substrate was placed in a bath of semiconductor grade acetic acid at 60 °C for 1 or 2 minutes to remove the native oxide layer. For some samples a final step of the cleaning process involved a second quick rinse in pure DI water at room temperature followed by drying with a flow of compressed UHP nitrogen.

Three gold plating precursor solutions were tested; their properties are summarized in table 1. Plating was performed by placing the precursor solution to be tested in a Pyrex beaker which was constantly stirred and heated to 60 °C. The substrate to be plated was held within the solution using a stainless steel alligator clip, which was a counter electrode to a platinum wire mesh cathode placed below the substrate. The mesh was contoured slightly around the bottom of the substrate but did not touch.

Table 1. Precursor solution and electroplating conditions used by NRC to deposit gold on copper.

Name	Supplier	Comments	Plating steps per period
TSG-250	Transene Company Danvers MA, USA	Sulfur containing, cyanide-free, neutral pH, sodium gold sulphite, sodium sulphite	0 mA, 35 ms 20 mA, 100 mV, 20 ms 0 mA, 35 ms -2 mA, 100 mV, 10 ms
SG-10	Transene Company Danvers MA, USA	Pure gold (99.99 %) plating, basic potassium aurocyanide solution	0 mA, 35 ms 20 mA, 100 mV, 20 ms 0 mA, 35 ms -2 mA, 100 mV, 10 ms
Orotemp 24	Technic Inc, Providence, RI, USA	Pure gold (99.9%) plating, neutral potassium aurocyanide solution	0 mA, 35 ms 10 mA, 100 mV, 20 ms 0 mA, 35 ms -1 mA, 100 mV, 10 ms

The plating waveform provided by a Keithley 6221 DC source was applied across the electrodes for 15 minutes after which time the sample was rotated 180° to prevent poor plating at the contact point of the electrode. After rotating, plating continued for another 15 minutes. The waveform used for plating consisted of a series of steps composed of a non-plating phase, a plating phase (20 mA, 100 mV, 20 ms), a second non-plating phase (0 mA, 35 ms), and a de-plating phase (-2 mA, 100 mV, 10 ms). This produces a smoother, more homogeneous film than would be expected from a single-phase plating signal. The resulting coating thickness for each sample was estimated to be about 1 µm -10 µm based on the expected deposition rate and time and the manufacturer's specifications.

The rankings for the precursor solutions are summarized in table 2. TSG-250 was ranked as the most suitable overall due to the apparent smoothness and relatively good homogeneity of the coatings it produced. Some pinholes were observed but did not cover the entire surface indicating that they might be controlled or eliminated with better substrate surface preparation. The plated film appeared amorphous and the topography observed appeared to be much less rough than the other precursors. The drawback of this precursor, not evaluated here, is the possible degassing of sulfur from the electrolyte which is a contaminant likely to be contained in the film. Sulfur has a relatively high vapour pressure and will degas in vacuum. This may perhaps be mitigated by vacuum annealing the substrate above the boiling point of sulfur.

The precursors SG-10 and Orotemp 24 both produce high-purity gold films but the latter is neutral in pH compared to the basic SG-10. Both electrolytes resulted in a gold film composed largely of crystalline particles, with those in the SG-10 derived film significantly larger than those in the Orotemp 24 derived one. This indicates that SG-10 would produce a much rougher surface than the other precursors tested; however, its homogeneity seemed the best, possibly because the large crystallite size and film thickness masked any underlying defects from being observed. It is not clear if the crystallite size and homogeneity of Orotemp 24 derived films would increase if the electroplating time and film thickness were increased. It appears possible that the poor film quality observed for this precursor is a result of a slower deposition rate and thus a thinner deposited film.

Table 2. Ranking of precursor electrolyte solutions based on SEM studies of the electroplated surfaces.

Precursor Trade Name	Roughness Rank	Homogeneity Rank	Comments	Overall Rank
TSG-250	1	2	Smooth likely amorphous surface with no obvious crystallite formation, some possible grain structure observed on the order of 100 nm. Small irregularly shaped pin holes 1 µm - 5 µm along the long axis observed in some locations. Sulfur content may degas in vacuum.	1
SG-10	3	1	Coating composed of large crystallites up to 2 µm along the long axis causing high surface roughness of similar magnitude assuming symmetry around the *x* and *z* directions. No pinholes obvious, high coverage even over defects. High-purity gold.	2
Orotemp 24	2	3	Smaller crystallite structure with a roughness estimated to be around 500 nm to 1 µm on a local scale. Coating deposited poorly along striations and cracks about 10 µm long and 100 nm wide appear at high magnification, possibly indicating poor tolerance to substrate imperfections. Coating 99.9 % pure.	2

2.2 HÄFNER GOLD-ELECTROPLATED AND RHODIUM-ELECTROPLATED COPPER SURFACES

The bulk material was oxygen free high conductivity copper (OFHC Cu) provided by EJPD. At the manufacturing site of Häfner, 12 mm diameter, 1 mm thick disc-shaped samples were machined and polished using the same polishing technique as that used to manufacture stainless steel weights. The surface roughness (S_a) of the copper samples following polishing was of the order of 10 nm. Subsequently, half of the samples were electroplated with (DUOR®, Au 99.8 %wt, Co 0.2 %wt) and the other samples were coated with Rh. The electroplating was conducted in collaboration with Fa. Umicore (former Degussa). The requirements were to coat the copper samples with a 2 µm layer of (non-magnetic) nickel and then to deposit a gold or rhodium layer with a thickness of between 0.5 µm and 1 µm.

3 HOMOGENEITY AND TOPOGRAPHY OF ELECTROPLATED COPPER SURFACES

The samples were analysed by scanning electron microscopy (SEM). The studies were performed in Finland at Aalto University, School of Chemical Technology, Department of Materials Science and Engineering. The instrument used was a Hitachi S-4700 cold field emission electron gun instrument equipped with a semi-in-lens detector. High resolution electron micrographs from the surfaces were taken at magnifications of x700, x20,000 and x70,000 utilizing low acceleration voltage (5 kV). Below are images of surfaces produced using different precursors.

3.1 TSG-250 PRECURSOR (NRC SAMPLES)

Scanning electron micrographs for a sample plated using precursor TSG-250 are presented in figure 1. The macro-scale homogeneity is best demonstrated in figure 1a in which the area shown is approximately 5 mm × 4 mm. The edge of the sample can be seen in the top left of the image with one major area of depleted plating seen near the centre of the image. Small pin holes can be seen over most of the surface but the concentration of pin holes is smaller at the left side of the image with the leftmost 1 mm showing almost no pinholes. This indicates that the number of pinholes might be reduced by optimizing the properties of the underlying substrate. In figures 1b and 1c the pinholes are shown in higher magnification and can be seen to vary in shape and are generally in the 1 µm - 5 µm size range. It is not clear if the pin holes extend right down to the underlying substrate but this would be likely if disruption of the electrochemical plating reaction occurred at these points due, for example, to the presence of an oxide or other defect. The striations particularly visible in figure 1b are remnants of the machining process, and could be largely eliminated through surface polishing of the underlying copper which can be produced with a near optical finish. Figure 1d demonstrates the lateral roughness of the highest frequency observed in the images, it is likely that this is due to either the grain structure of the gold over layer or the topography of an amorphous overlayer.

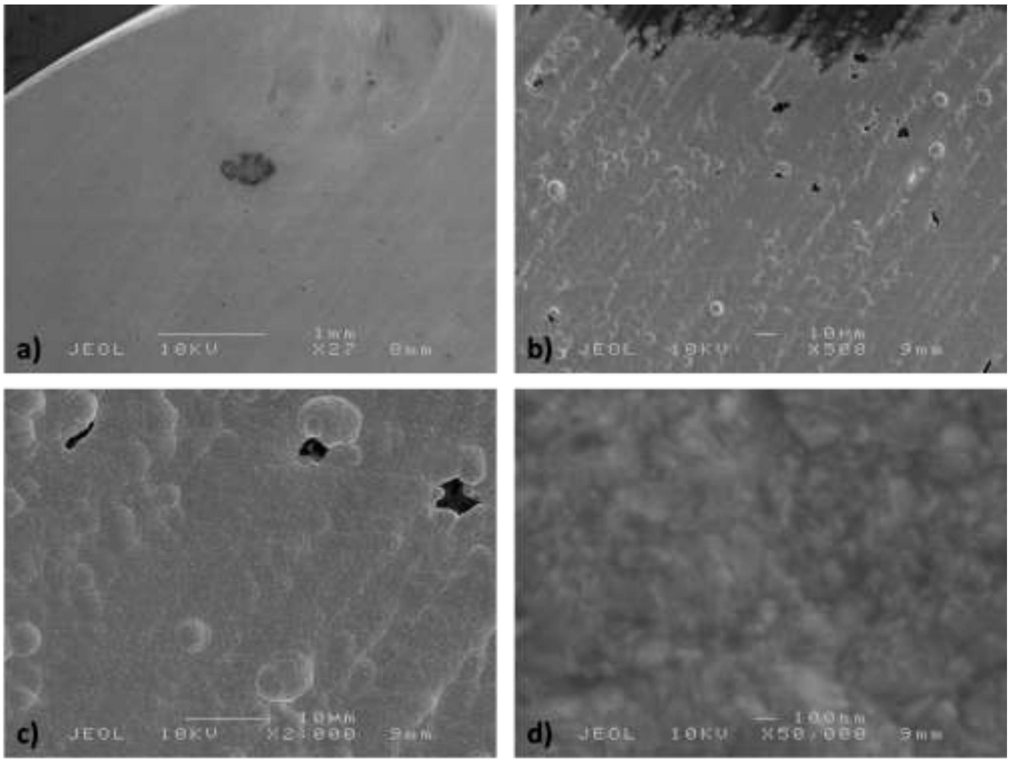

Figures 1a to 1d. SEM micrographs of NRC prepared samples demonstrating the lateral homogeneity and roughness of the gold plating formed from TSG-250 precursor solution on OFHC copper at NRC. The images a,b,c,d were each obtained at different magnifications (×27, ×500, ×2,000, ×50,000 respectively) as indicated by the incorporated scale bars in the image.

In figure 2 images of two different areas on the sample under the same imaging parameters are shown, at this scale some variation in the topography can be observed with the surface of figure 2a being slightly rougher than that of figure 2b. While SEM does not typically provide height information, the added contrast observed in figure 2a could indicate a higher vertical roughness when compared to figure 2b. The homogeneity observed in Figure 2b would be preferable for mass surfaces due to the smaller grain size and higher resulting smoothness. It is unclear if the difference observed between the regions shown in figures 2a and 2b are a consequence of the substrate inhomogeneity, local plating conditions or both, with some contribution due to changes in local imaging quality resulting from variable surface charging. Such conditions could be further explored to improve film quality.

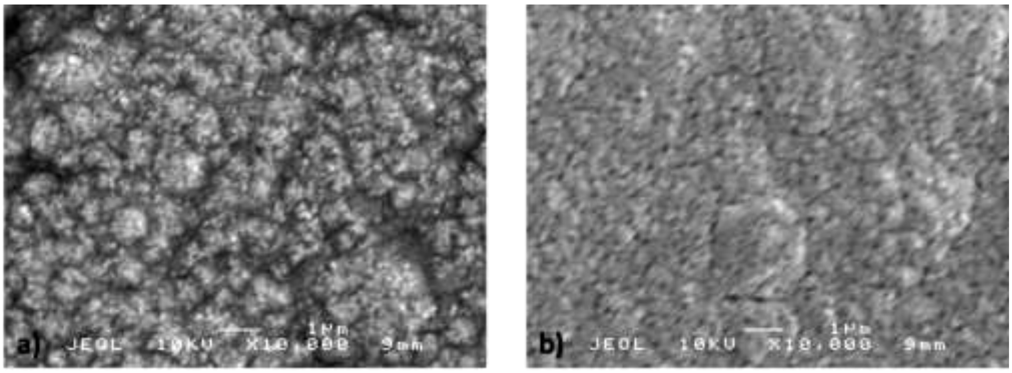

Figures 2a and 2b. (×10,000) Scanning electron micrographs of two random locations obtained under identical scan conditions. The difference between the images demonstrates the slight variation of surface structure with position. Au plated from TSG-250 precursor solution on OFHC copper at NRC.

3.2 SG-10 PURE GOLD (NRC SAMPLES)

Figure 3 shows scanning electron micrographs of gold plating using SG-10 as precursor at the same magnifications as presented in figure 1 a-c and figure 2. For this image set figure 3a shows a fairly homogeneous surface at low magnification except for a large defect near the left side likely arising due to surface defects of the substrate. At higher magnification crystallites begin to become apparent with the high contrast in figure 3c and 3d possibly indicating higher vertical roughness as compared to the surface produced using TSG-250 precursor. Moreover figure 3d and its inset show large crystalites in the 100 nm to 2 µm range along the long axis. The symmetry of the crystals indicates that the *Rz* roughness could be of the same order, though this is difficult to confirm via SEM. Interestingly, the dark region seen in figure 3b as imaged in higher magnification at the bottom left corner of figure 3d clearly demonstrates that the region is still coated and could appear darker due to reduced surface charge over the area or a variation in the chemistry of the plating material or perhaps the underlying substrate over the area. No pin holes are obvious in the images, though the shape of the crystalites makes absolute confirmation difficult.

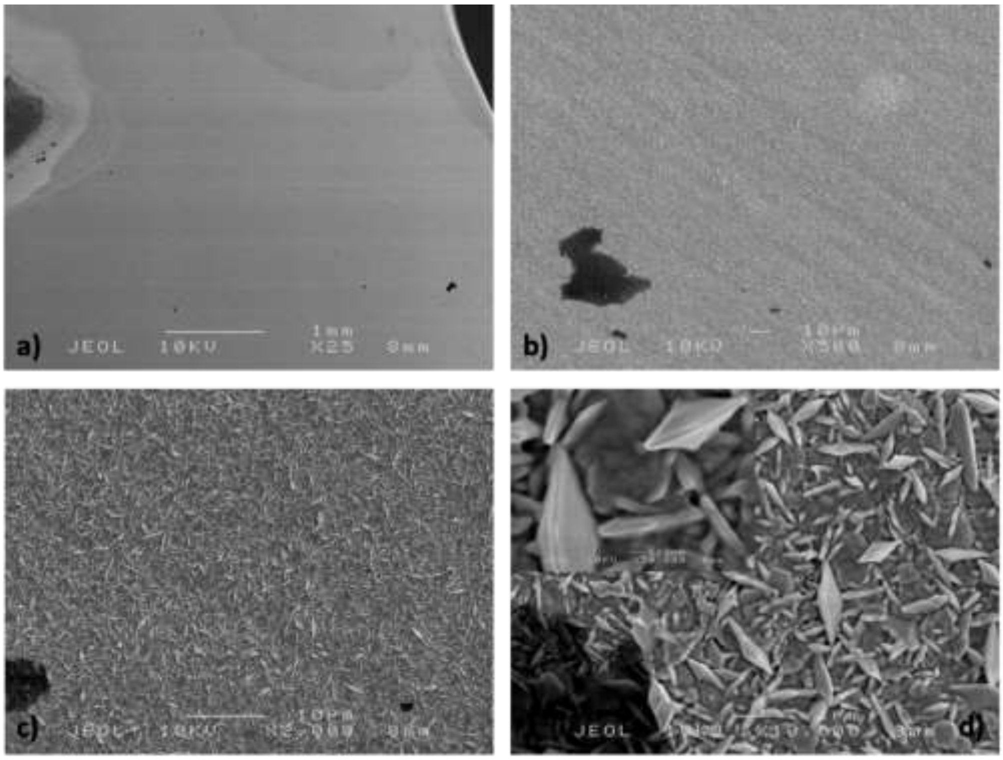

Figures 3a to 3d. Scanning electron micrographs acquired at NRC of gold electroplated OFHC copper substrates using SG-10 pure gold as a precursor. The magnifications and scales are shown in the images (×27, ×500, ×2,000, ×10,000, ×50,000 for figures a, b, c, d and the inset respectively) The coating is composed of crystallites with a range of sizes up to nearly 2 µm.

3.3 OROTEMP 24 PRECURSOR (NRC SAMPLES)

In figure 4 the SEM micrographs of electroplated gold on copper derived from commercial Orotemp 24 precursor is presented. These micrographs were acquired at the same magnification as those presented for the previous precursors. At the lowest magnification, no pin holes are observed as they were for precursor 1 and again a large defect, likely a result of the underlying substrate, is observed in the top left part of figure 4a. The surface otherwise appears quite homogeneous at this magnification. Pinholes become apparent in figure 4b with areas along the heaviest substrate striations showing poor coverage. Cracks in the surface coating are observed in figures 4c and 3d, with the underlying crystallite composition of the coating becoming especially apparent in figure 4d and its inset. The crystallites are significantly smaller than those observed in the coating produced from precursor 2 with the vast majority under 0.5 µm along the major axis. The crystallites are nominally the same shape as for precursor 2 and the *Rz* roughness not including the cracks or striations is estimated to lie between precursor 1 and 2. The smaller sized crystals could be a property of the coating or possibly a result of a lower deposition rate of the precursor that led to smaller amount of gold being deposited and a thinner coating. A thinner coating compared to precursors 1 and 2 could also explain the high number of defects observed especially if they derive from the underlying substrate. The influence of the substrate on the coating would be reduced with higher thickness.

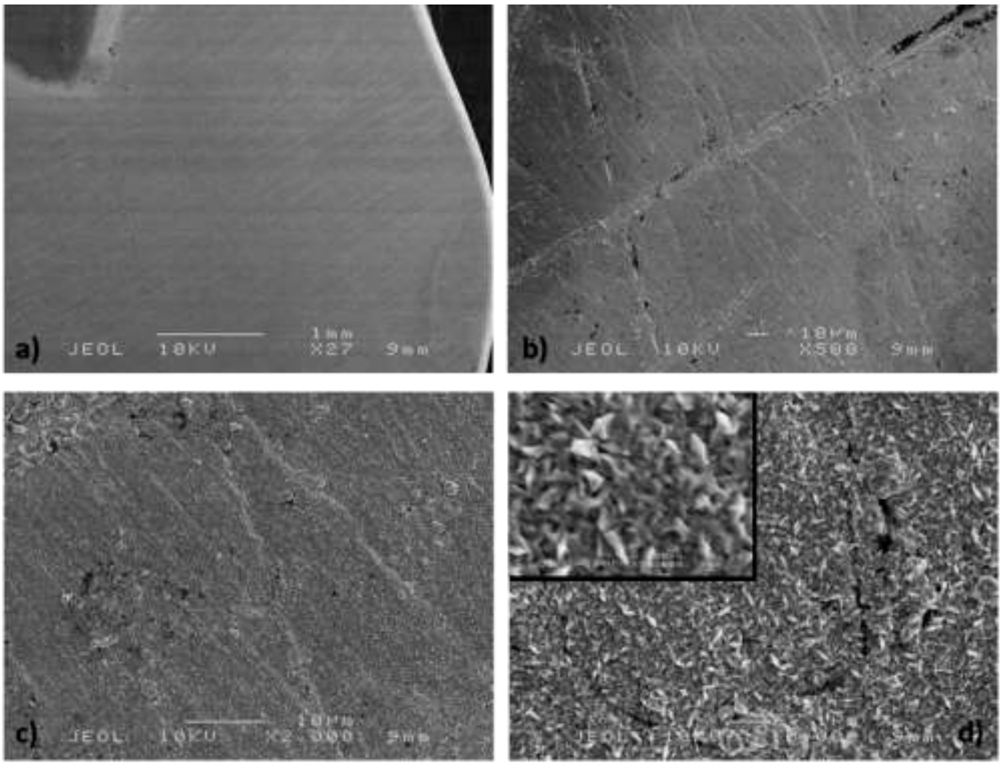

Figures 4a to 4d. Scanning electron micrographs of NRC gold electroplated OFHC copper substrates using Orotemp 24 pure gold as a precursor. The magnifications and scales are shown in the images (×27, ×500, ×2,000, ×10,000, ×50,000 for figures a, b, c, d and the inset respectively).

3.4 HÄFNER GOLD PLATED SURFACE

The Häfner gold plated samples were examined using X-ray Photoelectron Spectroscopy (XPS) and Atomic Force Microscopy (AFM) at MIKES. The gold surface was found smooth and homogenous indicating that the coating of the copper was successful (figures 5-7). Moreover, very little surface contamination and only single randomly oriented grooves were found. At higher magnifications the microstructure of the epitaxially grown gold film is clearly seen. The grain size of the film was about 500 nm.

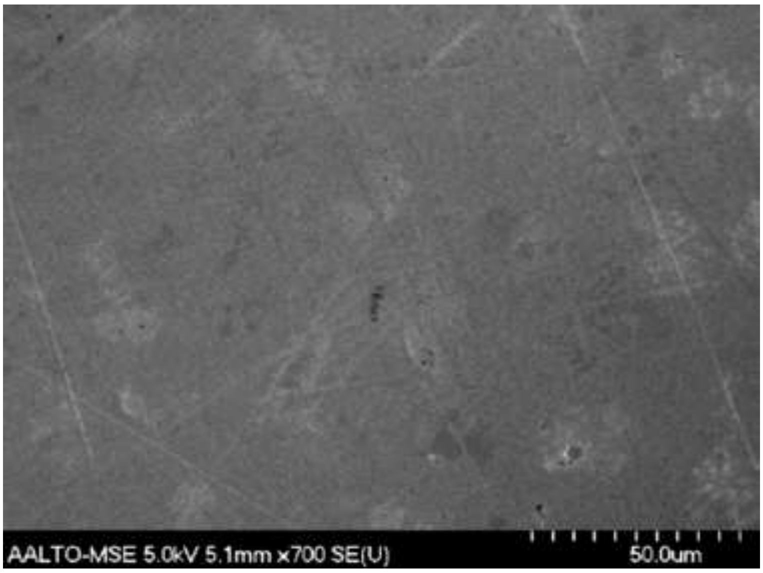

Figure 5. SEM micrograph at ×700 magnification of gold-electroplated copper surface produced by Häfner.

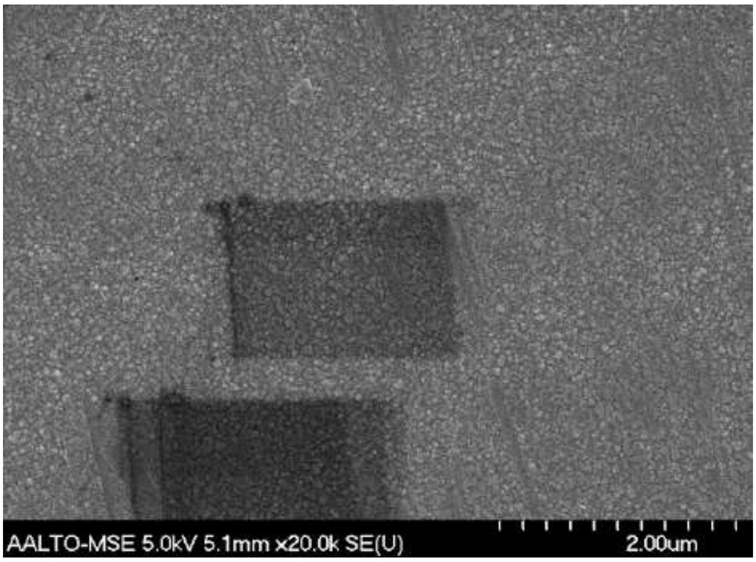

Figure 6. SEM micrograph at ×20,000 magnification of gold-electroplated copper surface produced by Häfner.

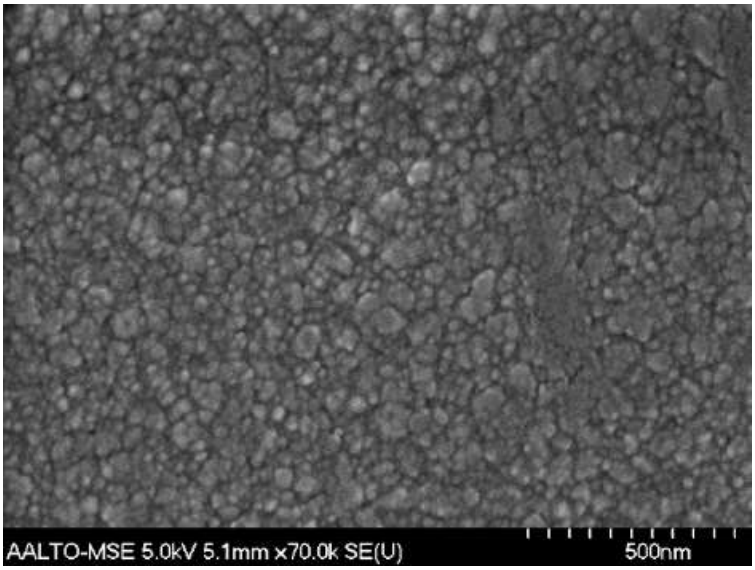

Figure 7. SEM micrograph at ×70,000 magnification of gold electroplated copper surface produced by Häfner.

The AFM images of gold-electroplated copper surface (figures 8 and 9) are similar to the SEM images. The surface coating was found to be homogenous with a grain size of about 500 nm similar to the sample studied with SEM. Also, the sample showed very little surface contamination.

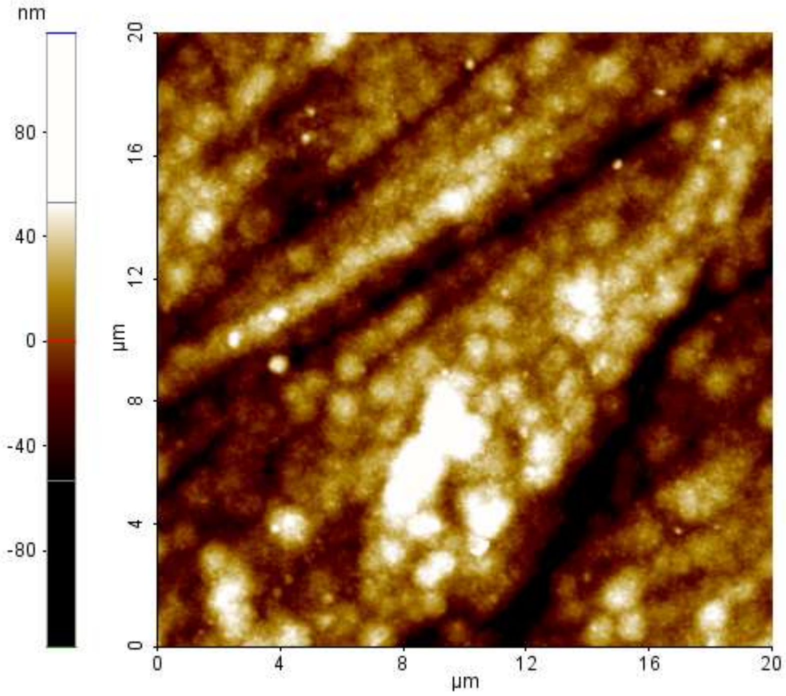

Figure 8. AFM topography image of gold-electroplated copper surface produced by Häfner, taken with a scan size of 20 µm × 20 µm.

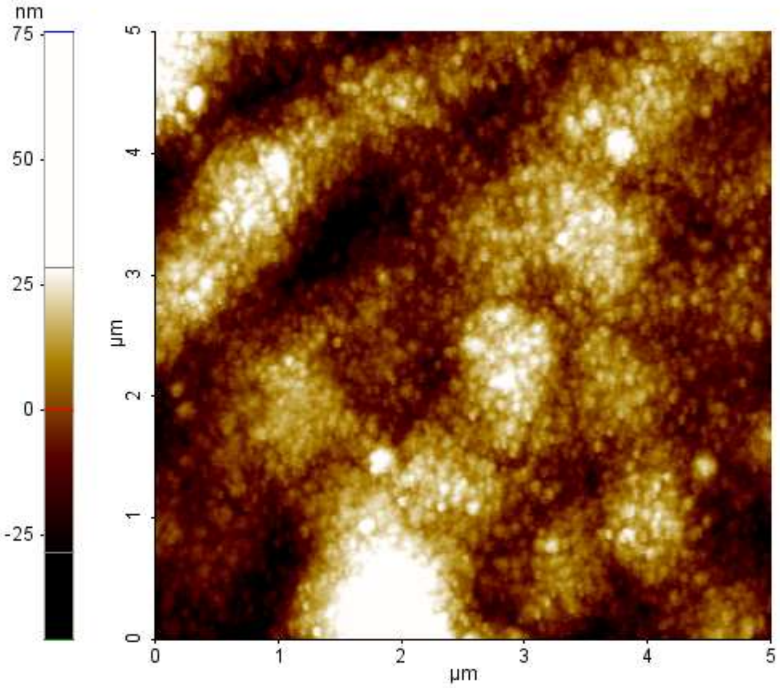

Figure 9. AFM topography image of gold-electroplated copper surface produced by Häfner, taken with a scan size of 5 µm × 5 µm.

The cleanliness and chemical composition of the samples was determined using XPS at EJPD. The instrument consists of an alpha110 detector and a twin anode x-ray source from Thermo Fisher Corp. All samples exhibited a natural contamination of roughly a monolayer of oxygen and carbon compounds, which is quite normal for samples exposed to ambient air. Beside this natural contamination the coating showed a homogenous gold spectrum. No other element species were detected. The extent of the carbonaceous surface contamination of the Häfner gold and rhodium plated samples (compared unplated metallic samples) before and after cleaning is shown in figure 15.

3.5 HÄFNER RH ELECTROPLATED COPPER SURFACE

The rhodium plated copper surface was also found to be homogenous and smooth (figures 10-12). Almost no surface contamination or grooves were found on the surface. Overall, the rhodium coating was found to be more homogenous than the gold coating. The grain size of the electroplated layer was less than 500 nm.

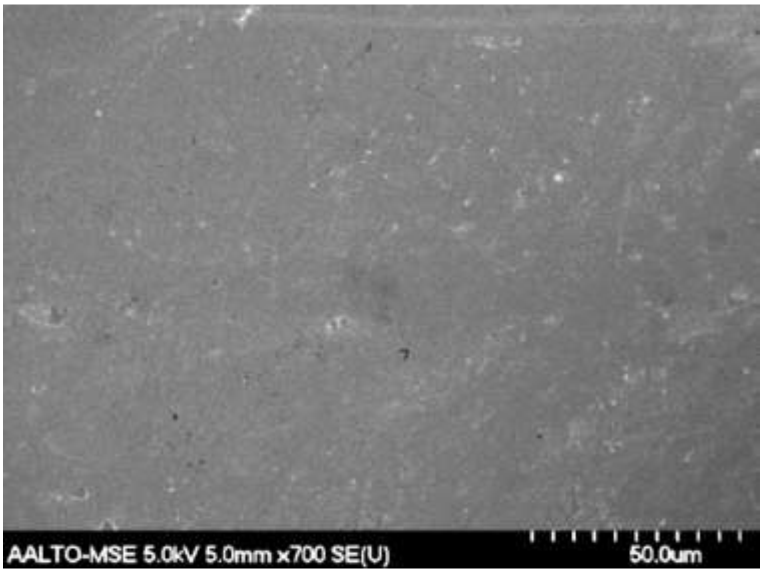

Figure 10. SEM micrograph at ×700 magnification of rhodium-electroplated copper surface produced by Häfner.

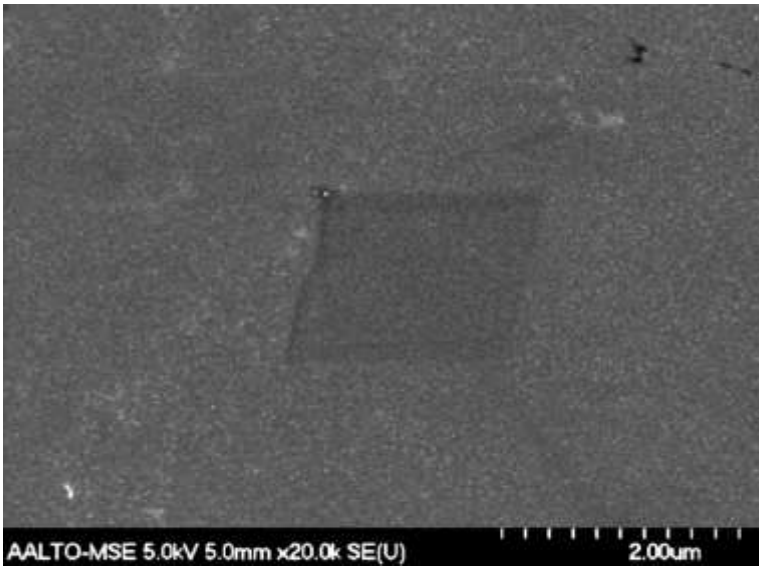

Figure 11. SEM micrograph at ×20,000 magnification of rhodium-electroplated copper surface produced by Häfner.

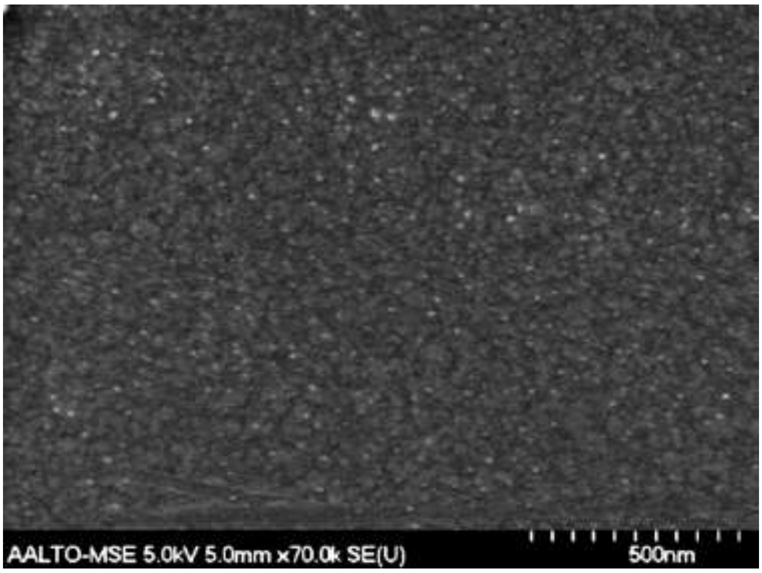

Figure 12. SEM micrograph at ×70,000 magnification of rhodium-electroplated copper surface produced by Häfner.

The rhodium-plated copper surface analysed with AFM was different from the sample analysed with SEM. Surface contamination and grooves were found contrary to the SEM analysed sample. However, the grain size was found to be similar to that of the SEM samples. From the SEM image with ×70,000 magnification (figure 12) and the AFM image with 5 µm × 5 µm scan size (figure 14) protuberances can be seen (as small bright dots). According to AFM analyses, these protuberances were about 50 nm in diameter and 5 nm high. They are probably not surface contamination but rather residual material left over from the coating process.

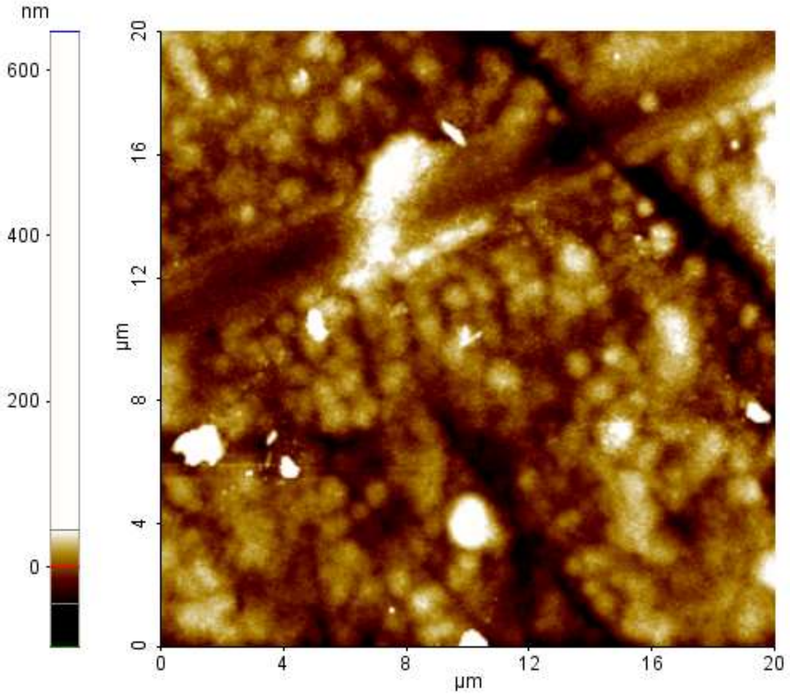

Figure 13. AFM topography image of rhodium-electroplated copper surface produced by Häfner, taken with a scan size of 20 × 20 µm.

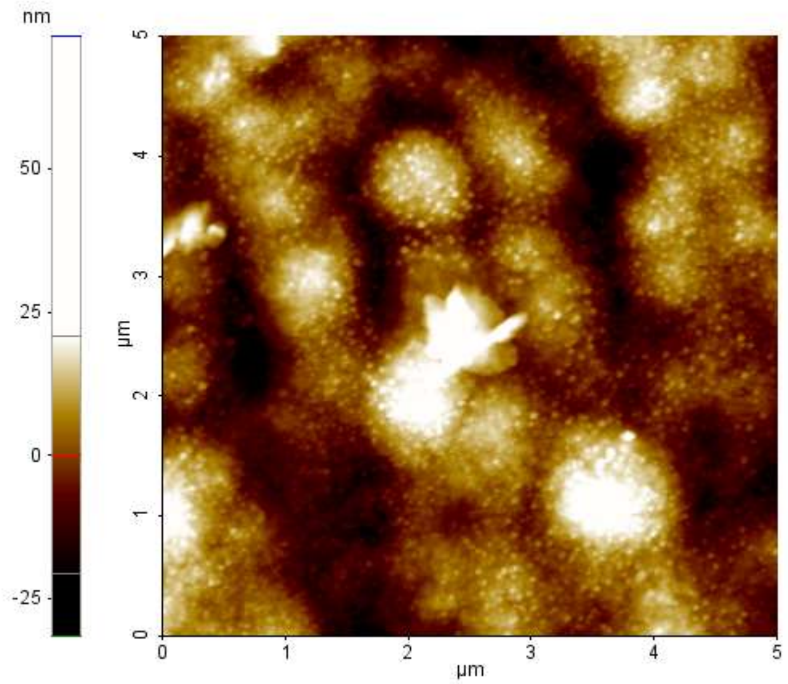

Figure 14. AFM topography image of rhodium-electroplated copper surface produced by Häfner, taken with a scan size of 5 × 5 µm.

The cleanliness and chemical composition of the samples was determined using XPS. The instrument consists of an alpha110 detector and a twin anode x-ray source from Thermo Fisher Corp. All samples exhibit significant contamination when compared with other (plated and metallic) samples tested. No other element species were detected. The extent of the carbonaceous surface contamination of the Häfner gold and rhodium plated samples (compared unplated metallic samples) before and after cleaning is shown in figure 15.

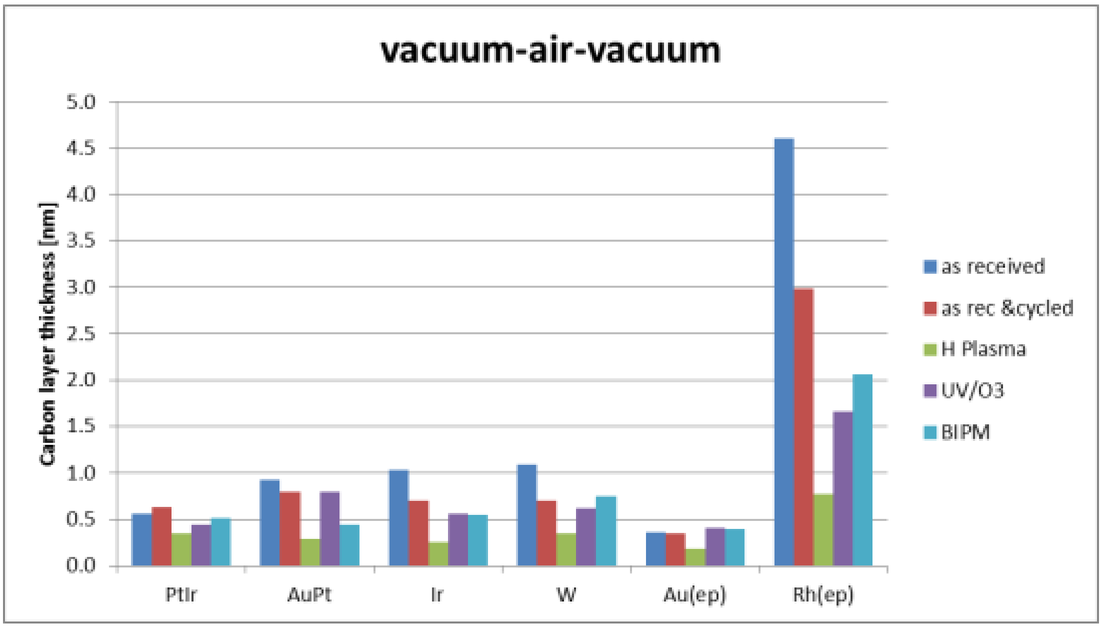

Figure 15. Carbon-layer thickness for different materials as received and after vacuum cycling and undergoing various cleaning processes.

The carbonaceous contamination shown in figure 15 indicates that, as received from Häfner, the gold plated surface showed slightly less carbonaceous contamination that the other non-plated materials. The rhodium plated surface had significantly more carbonaceous contamination some of which was removed (with various levels of effectiveness) by the individual cleaning processes identified. However, the residual carbon contamination was still greater than for the other samples.

4 COATING HARDNESS

The hardness of the Au and Rh coated samples prepared by Häfner was tested at the manufacturer site with a micro-indentation meter. Electroplated Au exhibits a hardness of 200 HV - 230 HV (Vickers) which makes it five times harder than pure bulk Au. For rhodium, a hardness of 600 HV - 900 HV was found. Consequently both coatings should be very resistant to wear and abrasion. Note that by contrast bulk Cu has a hardness of only 60 HV. Hence, if subjected to strong shocks the bulk Cu will be deformed causing the coating to be removed. If however the samples are handled with care, the Au and Rh coatings should be quite resistant to scratches.

5 ROUGHNESS CHARACTERISATIONS

The surface roughness was characterized using three different methods: laser scattering (Cnam), atomic force microscopy (MIKES) and white light scattering (EPJD). Figure 16 shows results obtained using the first method and presents mean power spectral density (PSD) of each sample analyzed in the spatial frequency range 0.1 μm^{-1} – 2.7 μm^{-1}. From these PSDs, the RMS height is extracted (see table 2). From the comparison of the PSDs, we can note that each material has a characteristic PSD shape and amplitude. PSD is a signature of the surface roughness in a given spatial frequency domain and provides information complementary to the RMS height values. PSDs amplitude are higher for Au (ep) and Rh (ep) compared with Ir, Udimet 720 and Si.

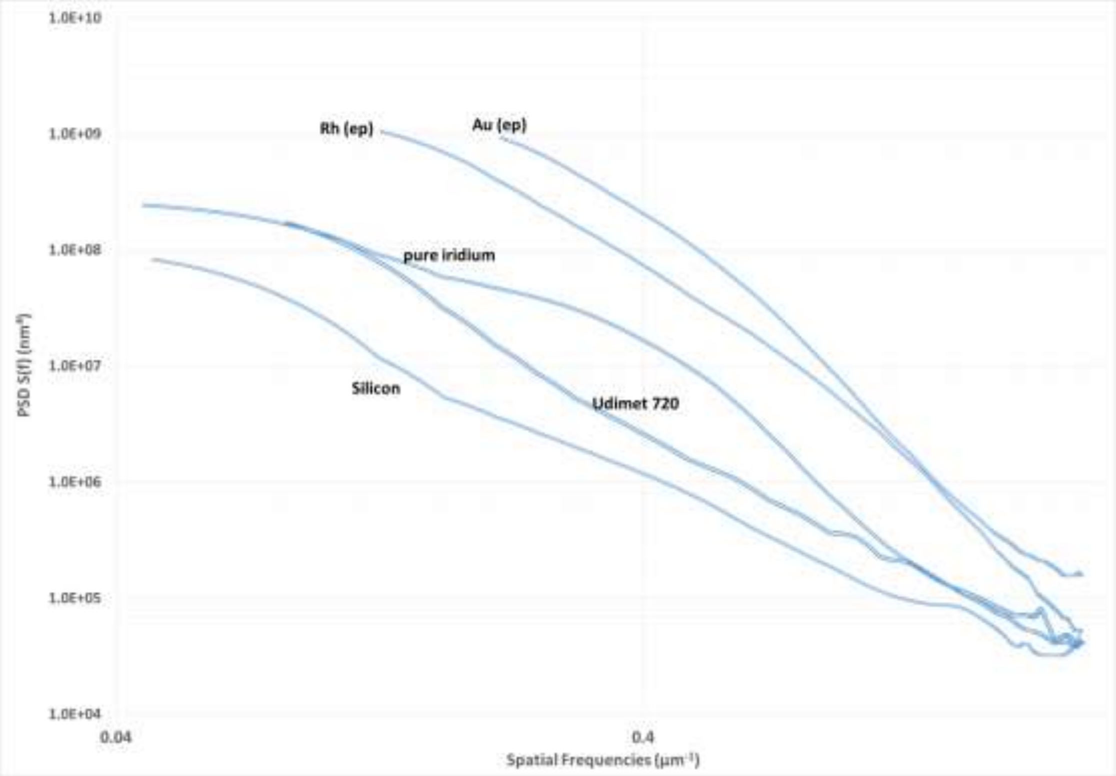

Figure 16. Laser scattering from different surfaces to measure roughness. Mean power spectral density curves for silicon, gold-electroplated copper Au(ep) and rhodium electroplated copper and Rh(ep). Comparison with iridium, silicon and Udimet 720. The PSD has dimensions of [L^4] as the scattering is two-dimensional. Specular reflection prevented measurements of the lowest spatial frequencies in some cases. See Zerrouki *et al.* [1] for more details.

EJPD performed comparative measurements via white light interferometry using a white light microscope (image size 718 µm × 546 µm). Primary Profile Filtering used a noise filter Cut-off, at λs = 2.5 µm. Measurements were made according to ISO 4287 with a cut-off wavelength, of 80 µm. The samples under investigation were cleaned using 3 cleaning techniques, BIPM *nettoyage-lavage* [2], UV Ozone [3] and H-plasma [4]. The results of the measurements (S_a) are shown in figures 17 to 19 (results from the solid materials investigated are also shown for comparison).

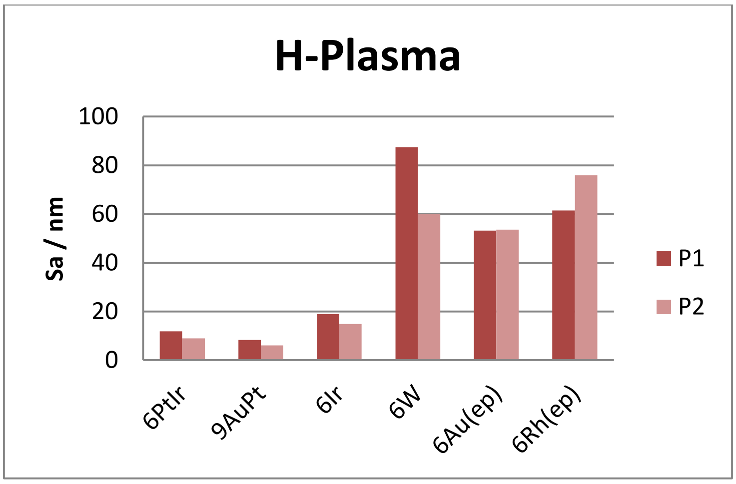

Figure 17. S$_a$ surface roughness values for H-plasma cleaned samples (measurements taken at 2 positions, P1 and P2, on the sample surface).

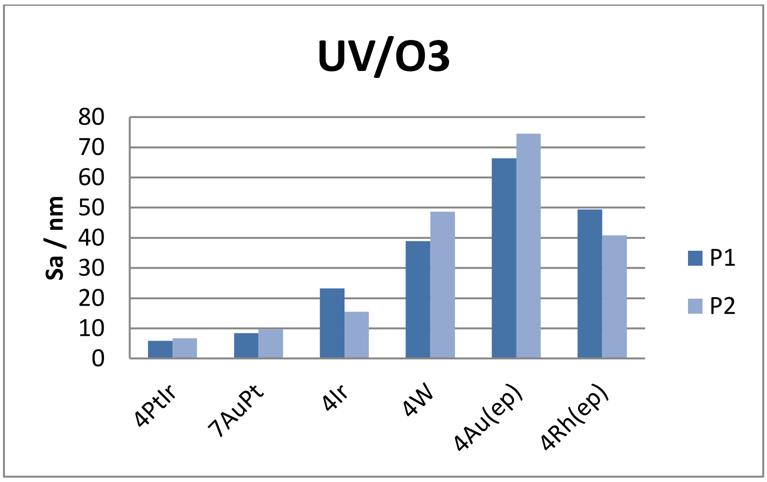

Figure 18. S$_a$ surface roughness values for UV/Ozone cleaned samples (measurements taken at 2 positions, P1 and P2, on the sample surface).

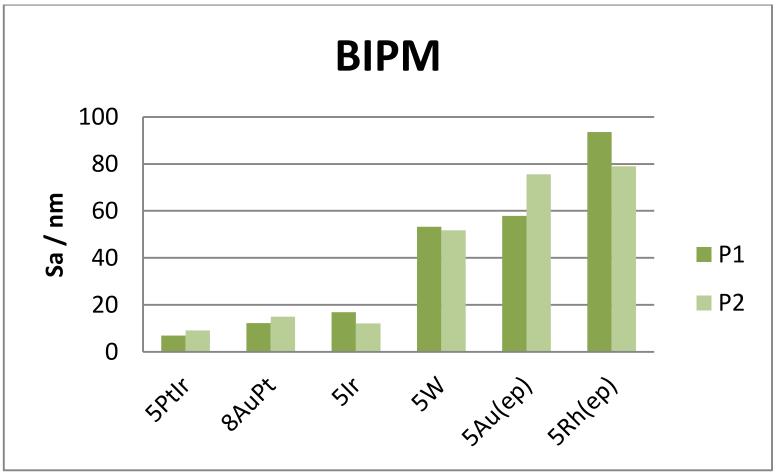

Figure 19. S$_a$ surface roughness values for samples cleaned by *nettoyage-lavage* (measurements taken at 2 positions, P1 and P2, on the sample surface).

Similar to the results from laser scattering, the results for the two plated samples (Au(ep) and Rh(ep)) measured with a white light microscope are significantly rougher than the samples produced from solid materials.

6 HUMIDITY AND PRESSURE CYCLING

Since the intention is for new mass standards to be comparable with use in air and vacuum the effect of humidity and pressure cycling in the integrity of the plated overlayers was assessed. Before initiating the vacuum/humidity cycles, two gold and two rhodium plated samples were surface mapped (total surface area for each sample of approximately 2 mm × 2 mm) and their surface roughness parameters measured with a confocal laser microscope using a ×50 optical lens. Five cycles were performed: the samples were cycled between vacuum (pressures of about 0.4 Pa) and atmospheric pressure at a relative humidity of about 60 %. The samples were left for about 1 hour in each environment. After the 5 cycles, the samples were again analysed using the same technique. Figure 20 shows the apparatus used for the vacuum/humidity cycling of the samples.

Figure 22. Apparatus used for vacuum/humidity cycling.

All four surface samples were examined. Figures 21 and 22 show images with a surface area of approx. 0.22 mm × 0.22 mm taken before and after cycling.

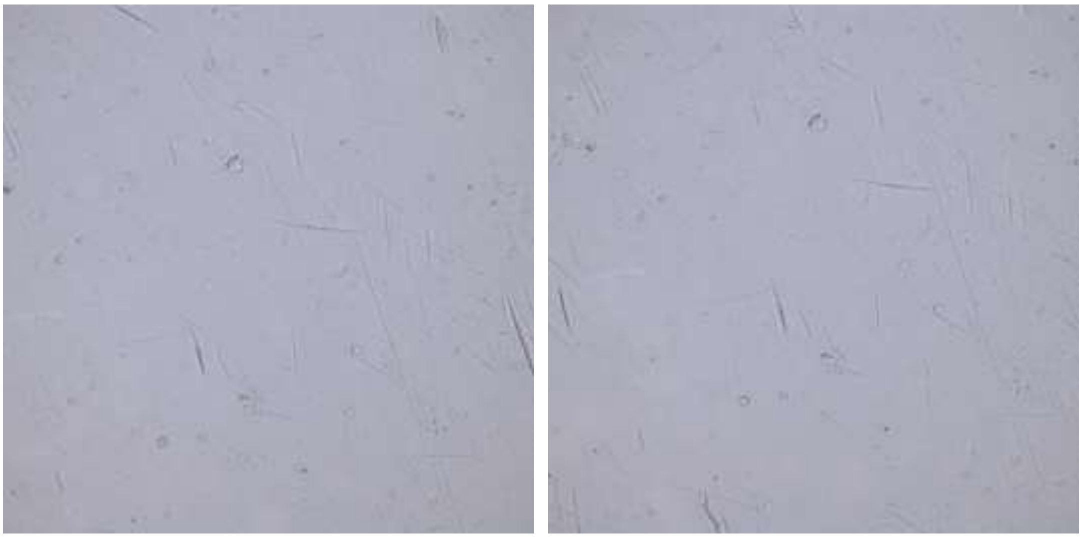

Figure 21. Rhodium plated sample before (left) and after (right) vacuum/humidity cycling.

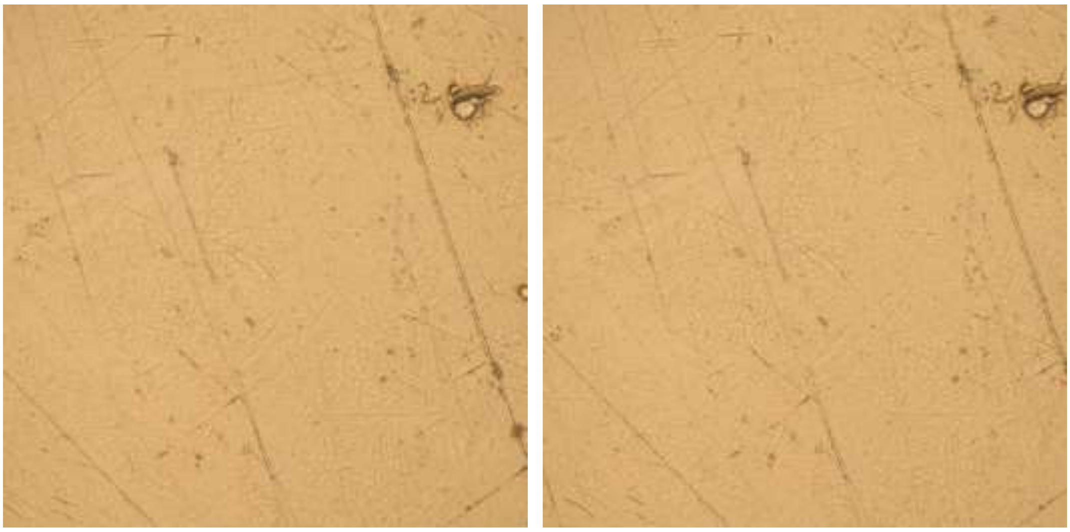

Figure 22. Gold plated sample before (left) and after (right) vacuum/humidity cycling.

Visually no changed in the surface were observed comparing the images before and after cycling. Table 3 summarise the surface roughness data acquired.

Table 3. Surface roughness (*Sa* and *Sq*) for rhodium plated and gold plated samples before and after vacuum/humidity cycling (measure by confocal microscopy).

Sample	**Before vacuum/humidity cycling**		**After vacuum/humidity cycling**	
	Sa / µm	*Sq* / µm	*Sa* / µm	*Sq* / µm
Rh_a0	0.021	0.049	0.022	0.050
Rh_a1	0.025	0.046	0.026	0.049
Au_b0	0.030	0.056	0.031	0.056
Au_b1	0.033	0.060	0.033	0.061

Within the uncertainty of the measurement (estimated as approximately ± 0.01 µm for both parameters when comparing measurements made on nominally the same area) no change in the surface parameters was seen.

7 THERMAL CYCLING

Although thermal cycling of (plated) mass standards is not envisaged in normal use following the vacuum/humidity cycling test the apparatus shown in figure 20 was also used to thermally cycle the samples. As before the samples were surface mapped (total mapped each sample approximately 2 mm × 2 mm). Five thermal cycles were performed in which the samples were subjected to a maximum temperature of about 160 °C for about one hour then cooled back to ambient temperature (about 20 °C). Heating the samples to 160 °C from ambient took approximately 30 minutes and the cooling took 2-3 hours.

All four surface samples were examined. Figures 23 and 24 show images with a surface area of approx. 0.22 mm × 0.22 mm taken before and after cycling.

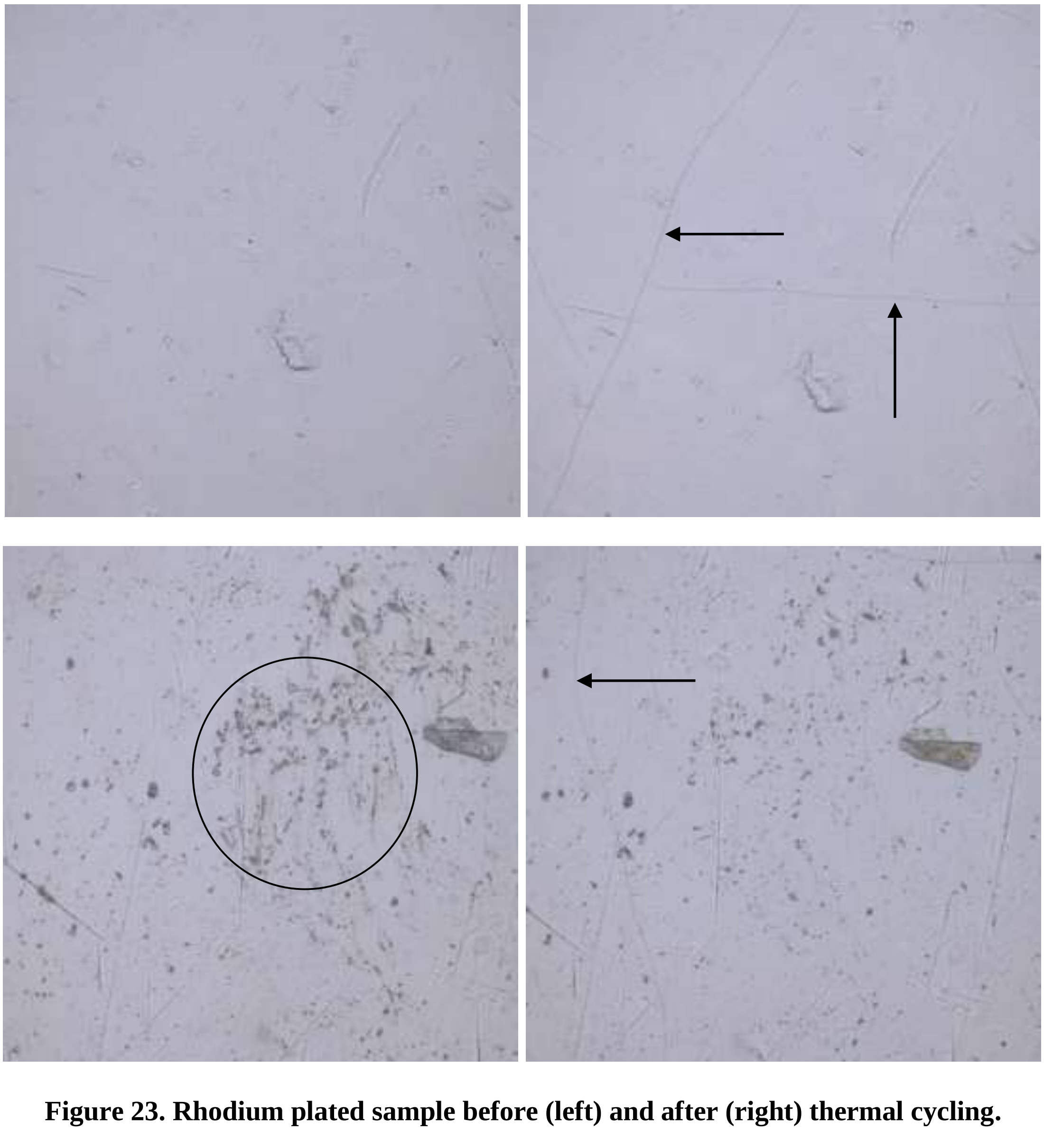

Figure 23. Rhodium plated sample before (left) and after (right) thermal cycling.

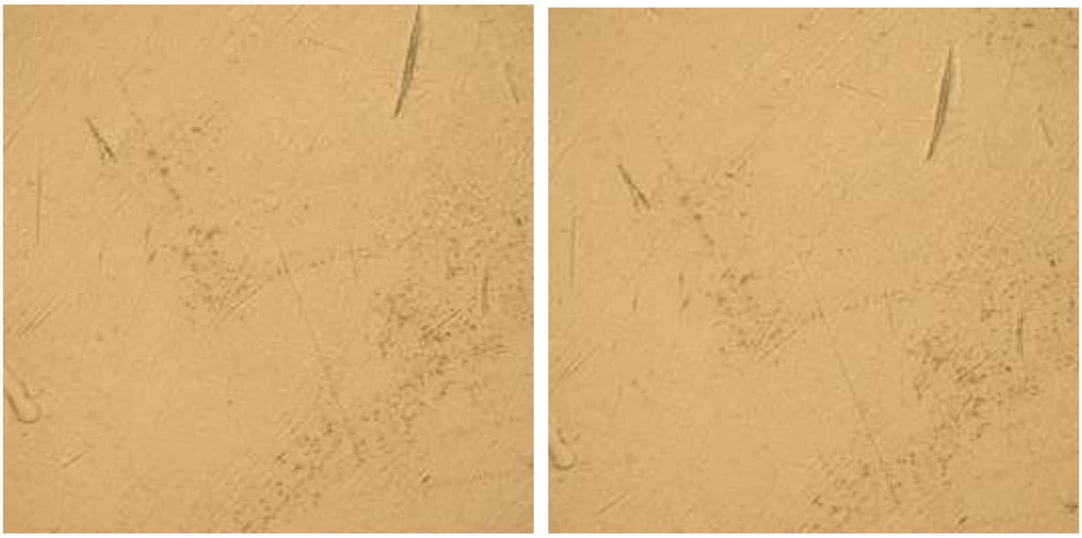

Figure 24. Gold plated sample before (left) and after (right) thermal cycling.

The two rhodium scans show additional fine cracks following thermal cycling (indicated by the arrows in the right hand images). The images following thermal cycling also indicate that the samples are significantly cleaner, illustrated by the removal of contamination (circled) from the before cycling sample area. This is due to the thermal desorption of surface contamination during the thermal cycling process.

The gold samples show no additional cracks after thermal cycling but again the post-cycling images show slightly cleaner surfaces.

Table 4 summarises the surface roughness measurements before and after thermal cycling for the two plating materials.

Table 4. Surface roughness (*Sa* and *Sq*) for rhodium plated and gold plated samples before and after thermal cycling (measure by confocal microscopy).

Sample	Before thermal cycling		After thermal cycling	
	***Sa* / µm**	***Sq* / µm**	***Sa* / µm**	***Sq* / µm**
Rh_a0	0.029	0.067	0.029	0.084
Rh_a1	0.018	0.036	0.018	0.038
Au_b0	0.036	0.076	0.042	0.090
Au_b1	0.035	0.074	0.044	0.087

Surface roughness values for the samples are slightly higher following thermal cycling, this is almost certainly a function of the thermal desorption of contamination from the samples exposing underlying scratches in the surface.

8 SUMMARY AND CONCLUSIONS

The roughness values for the plated materials provided by Häfner were significantly higher than for the other (unplated) materials studied in T 1.1.4 [5]. A granular surface structure was observed for plated surfaces with a grain size of 500 nm or less. Roughness measurements using white light reflection support these findings. Table 5 summarizes the surface roughness measurements from Cnam, MIKES and EJPD the results for measurement on samples of (pure) iridium are included form comparison. While the surface roughness values are not directly comparable they can be used to assess the relative (roughness) quality of the surfaces identified.

Table 5: Surface roughness (RMS height, *Rq* and *Sa*) of studied materials obtained using optical roughness meter, AFM and white light interferometry.

Optical roughness meter [0.1 – 2.7] µm^{-1}		**Atomic Force Microscope**		**White Light Microscope**	
Sample	**RMS height / nm**	**Sample**	***Rq* / nm**	**Sample**	***Sa* / nm**
Au (ep)	17 ± 0.6	Au (ep)	15 - 30	Au (ep)	60 - 70
Rh (ep)	10 ± 0.4	Rh (ep)	10 - 22	Rh (ep)	50 - 80
Ir (18-20)	4.6 ± 0.2	Ir 12	1.5 - 2.0	Ir (4-6)	15

The results show that the roughness of the plated samples was approximately 5 times greater that achieved on the iridium (and other uncoated metal) samples. However this is still significantly better than the surface finish required for OIML Class E1 weights [6].

Vacuum and humidity cycling had no measurable effect on the surface of the weights confirming the robustness of the coatings to variations in pressure and humidity experience on transfer between air and vacuum. After thermal cycling (20 °C to 160 °C) the rhodium plated sample showed additional cracks, whereas the gold samples were unaffected in this respect. This is likely to be caused by the difference in the (linear) thermal expansion coefficients of the rhodium and the copper substrate (8 ppm per °C for rhodium compared with 16.6 ppm per °C for copper). Gold and copper are much better matched in term of their linear thermal expansion coefficients (14.2 ppm and 16.6 ppm per °C respectively). Additionally rhodium has a poorer thermal conductivity than gold or copper (150 $W \cdot m^{-1} \cdot K^{-1}$ compared with 320 $W \cdot m^{-1} \cdot K^{-1}$ for gold and 390 $W \cdot m^{-1} \cdot K^{-1}$ for copper). An additional effect of the thermal cycling was the desorption of contaminants from the surface of the samples which could be seen visually and by a slight increase in the surface roughness parameters due to the exposure of roughness (scratches) underlying the contaminant overlayer.

REFERENCES

[1] C. Zerrouki, F. Miserey and P. Pinot, "Light scattering angular distribution of a mirror-polished CoCr20WNi (alacrite XSH); application to the determination of statistical parameters characterizing the surface roughness," Eur. Phys. J. Appl. Phy., 1, pp. 253–259, 1998.

[2] G. Girard, "The Washing and Cleaning of Kilogram Prototypes at the BIPM" (Sèvres: BIPM) (1990).

[3] K. Marti, P. Fuchs and S. Russi. "Cleaning of mass standards: a comparison of new and old techniques", Metrologia, 49,628 (2012).

[4] J. Berry, S. Downes and S. Davidson, "UV/ozone cleaning of platinum/iridium kilogram mass prototypes", Metrologia, 47, 410 (2010).

[5] EMRP SIB-05 Work Package 1, Deliverable 1.1.4, Summary report of properties of materials for potential use as mass transfer standards.

[6] OIML R 111-1 Edition 2004 (E) Weights of classes E1, E2, F1, F2, M1, M1–2, M2, M2–3 and M3, Part 1: Metrological and technical requirements.